

Selective Ammoximation of Ketones via In Situ H_2O_2 Synthesis

Richard J. Lewis,* Kenji Ueura, Xi Liu,* Yukimasa Fukuta, Tian Qin, Thomas E. Davies, David J. Morgan, Alex Stenner, James Singleton, Jennifer K. Edwards, Simon J. Freakley, Christopher J. Kiely, Liwei Chen, Yasushi Yamamoto, and Graham J. Hutchings*



Cite This: *ACS Catal.* 2023, 13, 1934–1945



Read Online

ACCESS |



Metrics & More



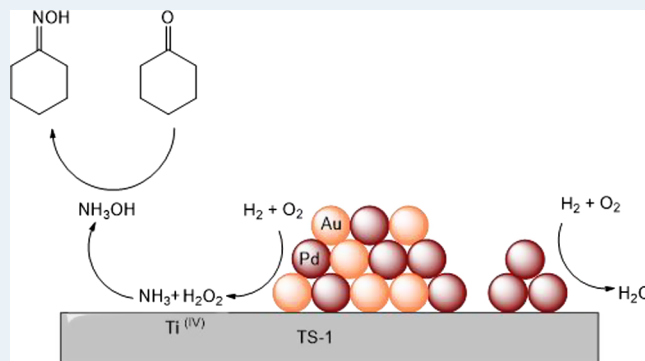
Article Recommendations



Supporting Information

ABSTRACT: The ammoximation of ketones to the corresponding oxime via the in situ production of H_2O_2 offers a viable alternative to the current means of industrial-scale production, in particular for the synthesis of cyclohexanone oxime, a key precursor to Nylon-6. Herein, we demonstrate that using a bifunctional catalyst, consisting of Pd-based bimetallic nanoparticles immobilized onto a TS-1 carrier, it is possible to bridge the considerable condition gap that exists between the two key distinct reaction pathways that constitute an in-situ approach (i.e., the direct synthesis of H_2O_2 and ketone ammoximation). The formation of PdAu nanoalloys is found to be crucial in achieving high reactivity and in promoting catalytic stability, with the optimal formulation significantly outperforming both alternative Pd-based materials and the monometallic Pd analogue.

KEYWORDS: green chemistry, industrial catalysis, feedstock valorization, ketone ammoximation, hydrogen peroxide, palladium–gold



INTRODUCTION

Since first developed by EniChem,¹ the combination of the titanosilicate TS-1 and preformed H_2O_2 has found significant application in the chemical synthesis sector,² achieving excellent activities and selectivities for aromatic hydroxylation,³ the oxidative dehydrogenation of alkanes,⁴ and alkene epoxidation.⁵ The most pertinent examples of major industrial processes that utilize commercial H_2O_2 in conjunction with TS-1 are perhaps the integrated hydrogen peroxide to propylene oxide process^{6,7} and the ammoximation of cyclohexanone to cyclohexanone oxime,⁸ a key precursor in the production of the polyamide Nylon-6. With global demand for Nylon-6 estimated to reach approximately 9 million tons per annum by 2026,⁹ largely driven by its application as an industrial fiber and textile, a concurrent rise in cyclohexanone oxime production is likewise expected.¹⁰

The conventional approach to cyclohexanone oxime manufacture, which reacts cyclohexanone with hydroxylamine salts, is considered to be highly inefficient, producing large quantities of low-value byproducts, such as ammonium sulfate.^{11,12} However, the development of the EniChem route, which combines TS-1 with preformed H_2O_2 in conjunction with ammonia, largely overcame these efficiency concerns, achieving selectivities toward the oxime typically in excess of 95%.^{13,14} It is widely considered that the H_2O_2 /TS-1 route proceeds via an intermediate hydroxylamine species, which is synthesized over the Ti^{IV} sites present within the

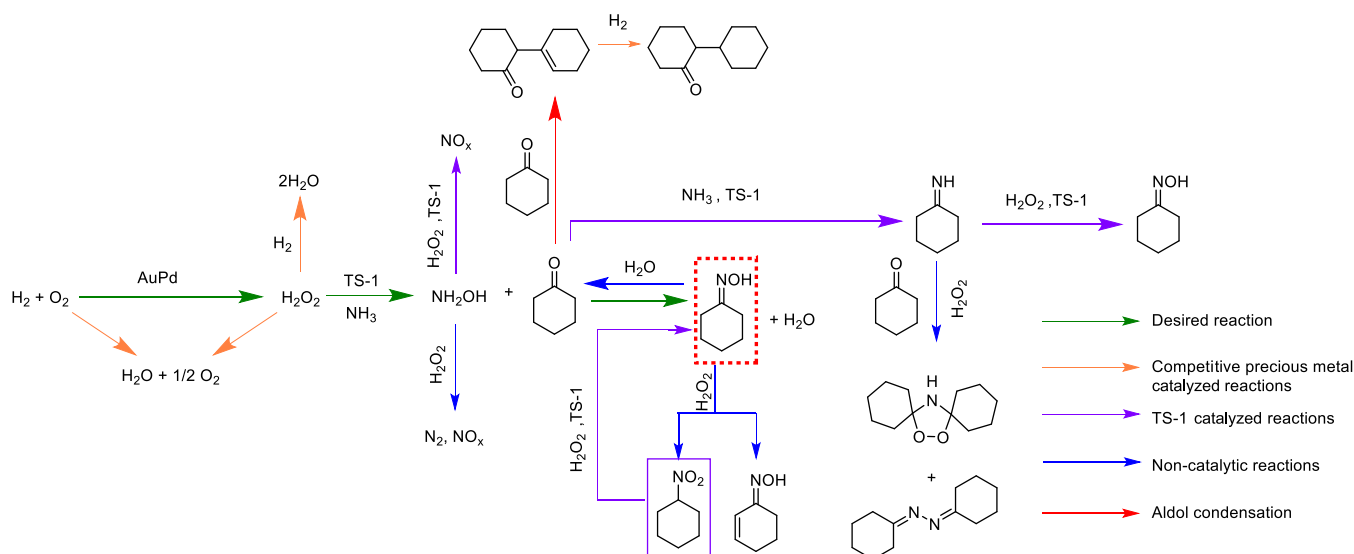
titanosilicate framework.¹⁵ This subsequently reacts non-catalytically with cyclohexanone to produce the oxime. Despite the high oxime selectivity and efficiency of the industrial ammoximation process, the addition of preformed H_2O_2 in stoichiometric excess is typically required,¹⁶ due to its poor stability under ammoximation reaction conditions, namely, elevated temperatures (≥ 80 °C) and the high pH of the reaction solution, resulting in an associated increase in process costs.

Furthermore, the industrial route to cyclohexanone oxime is hampered by the considerable economic and environmental drawbacks associated with the means by which H_2O_2 is produced on an industrial scale, the anthraquinone oxidation process, which accounts for approximately 95% of global H_2O_2 production.¹⁷ These include low atom efficiency and high infrastructure costs, with the latter often dictating that H_2O_2 production is prohibited at the point of use and necessitating the transport and storage of H_2O_2 at concentrations far in excess of that required by the end user, with the energy utilized in the concentration process effectively wasted when H_2O_2 is

Received: November 25, 2022

Revised: January 4, 2023

Scheme 1. Proposed Reaction Scheme for the Ammoxidation of Cyclohexanone to the Corresponding Oxime, via In Situ H_2O_2 Synthesis



diluted to desirable concentrations.^{18,19} In addition, the instability of H_2O_2 at temperatures which can be considered to be relatively mild requires the use of propriety stabilizing agents to prevent decomposition to H_2O during transport and storage and prolong shelf-life. Such additives can promote reactor corrosion, limit catalyst lifetime, and result in complex product streams, adding further cost to any industrial process that utilized preformed H_2O_2 .²⁰ Likewise, all systems that utilize commercial H_2O_2 can be considered to suffer from these same inefficiencies to a certain extent.

The decoupling of oxidative transformations, such as cyclohexanone ammoxidation, from off-site H_2O_2 production, would potentially lead to considerable economic savings and a reduction in greenhouse gas emissions, representing a positive step toward more sustainable industrial processes. To this end, several studies have investigated the efficacy of alternative approaches that would avoid large-scale H_2O_2 production and allow for the on-site production and direct utilization of H_2O_2 . However, to date, these systems have not been simple or robust enough for adoption on an industrial scale. For example, the supply of H_2O_2 via the partial oxidation of isopropanol as described by Liang et al.²¹ and Zajacek et al.²² yields appreciable concentrations of impurities, producing an undesirable and complex product mixture. By comparison, the in situ production of H_2O_2 from molecular H_2 and O_2 would negate the significant drawbacks associated with commercially synthesized H_2O_2 , while avoiding the dilution of product streams through the continual addition of an aqueous oxidant and could offer an overall reduction in process costs.

A proposed reaction for the ammoxidation of cyclohexanone via in situ H_2O_2 synthesis is outlined in Scheme 1 and can be considered to be comparable to the current industrial process where the preformed oxidant is continually supplied.¹ In the case of the in situ approach, immobilized precious metal species are responsible for the formation of the oxidant, which is subsequently utilized in the formation of hydroxylamine by Ti^{IV} sites present within the TS-1 framework, with the intermediate species subsequently reacting noncatalytically with the ketone to synthesize the correspond-

ing oxime. In order to achieve maximal process efficiency, there is clearly a need to balance the rate of H_2O_2 synthesis over the metal component with that of hydroxylamine formation and inhibit competitive H_2O_2 degradation reactions catalyzed by metal species, which limits selective utilization of H_2 .

We have recently demonstrated that it is possible to achieve high selectivities toward cyclohexanone oxime production via the in situ synthesis of H_2O_2 ,²³ overcoming the considerable condition gap that exists between these two critical processes, with the direct synthesis of H_2O_2 favored by acidic conditions^{24–26} and sub-ambient temperatures,²⁷ while cyclohexanone ammoxidation is associated with elevated temperatures (80–140 °C) and utilizes ammonia. Building on this previous study, which focused extensively on a tandem system, consisting of a H_2O_2 synthesizing catalyst used in conjunction with a commercially available TS-1, we now focus on a composite bifunctional catalyst, that is able to both synthesize H_2O_2 and subsequently utilize the oxidant in the production of cyclohexanone oxime.

EXPERIMENTAL SECTION

Catalyst Preparation. Mono- and bi-metallic 0.66%Pd–X/TS-1 [where Pd:X = 1:1 (wt/wt) and X = Au, Pt, Ni, Cu, Rh, Ir, Co, Mn, Ga, Ag, Sn, Ru, and In] catalysts have been prepared by a wet co-impregnation procedure, based on a methodology previously reported in the literature.²⁸ The procedure to produce the 0.33%Pd–0.33%Au/TS-1 catalyst (2 g) is outlined below with a similar methodology utilized for all mono- and bimetallic analogues. The requisite amounts of metal precursor used for the synthesis of key catalysts is reported in Table S1.

PdCl_2 (1.100 mL, [Pd] = 6.00 mgmL^{-1} , Sigma Aldrich) and $\text{HAuCl}_4 \cdot 3\text{H}_2\text{O}$ (0.539 mL, [Au] = 12.25 mgmL^{-1} , Strem Chemicals) were charged into a 50 mL round bottom flask, with total volume adjusted to 16 mL using H_2O (HPLC grade, Fischer Scientific). The resulting mixture was heated to 65 °C in a thermostatically controlled oil bath with stirring (600 rpm). Upon reaching the requisite temperature, TS-1 (1.987 g, HighChem) was added over the course of 5 min. The resulting slurry was subsequently heated to 85 °C for 16 h to allow for

complete evaporation of water. The resulting solid material was ground prior to calcination in static air (typically 400 °C, 3 h, 10 °C min⁻¹).

Catalyst Testing. Note 1: Reaction conditions used within this study operate below the flammability limits of gaseous mixtures of H₂ and O₂.

Note 2: The conditions used within this work for H₂O₂ synthesis and degradation have previously been investigated, with the use of sub-ambient reaction temperatures, CO₂ reactant gas diluent, and a methanol co-solvent identified as key to maintaining high catalytic efficacy toward H₂O₂ production.²⁷

Note 3: In all cases, reactions were run multiple times, over multiple batches of catalyst, with the data presented an average of these experiments.

Direct Synthesis of H₂O₂. Hydrogen peroxide synthesis was evaluated using a Parr Instruments stainless-steel autoclave with a nominal volume of 100 mL, equipped with a PTFE liner and a maximum working pressure of 2000 psi. To test each catalyst for H₂O₂ synthesis, the autoclave was charged with a catalyst (0.01 g) and solvent (5.6 g of MeOH and 2.9 g of H₂O, both HPLC grade, Fischer Scientific). The charged autoclave was then purged three times with 5% H₂/CO₂ (100 psi) before filling with 5% H₂/CO₂ (420 psi), followed by the addition of 25% O₂/CO₂ (160 psi) to give a H₂:O₂ ratio of 1:2. All pressures are provided as gauge pressures, and reactant gases were not continuously introduced into the reactor. The temperature was then decreased to 2 °C (using a HAAKE K50 bath/circulator and an appropriate coolant) followed by stirring (1200 rpm) of the reaction mixture for 0.5 h. H₂O₂ productivity was determined by titrating aliquots of the final solution after reaction with acidified Ce(SO₄)₂ (0.01 M) in the presence of a ferroin indicator.

Degradation of H₂O₂. Catalytic activity toward H₂O₂ degradation (via hydrogenation and decomposition pathways) was determined in a manner similar to that used for measuring the H₂O₂ direct synthesis activity of a catalyst. The autoclave was charged with methanol (5.6 g, HPLC grade, Fisher Scientific), H₂O₂ (50 wt % 0.69 g, Merck), H₂O (2.21 g, HPLC grade, Fisher Scientific), and catalyst (0.01 g), with the solvent composition equivalent to a 4 wt % H₂O₂ solution. From the solution, two aliquots of 0.05 g were removed and titrated with acidified Ce(SO₄)₂ solution using ferroin as an indicator to determine an accurate concentration of H₂O₂ at the start of the reaction. The charged autoclave was then purged three times with 5% H₂/CO₂ (100 psi) before filling with 5% H₂/CO₂ (420 psi). All pressures are provided as gauge pressures, and reactant gases were not continuously introduced into the reactor. The reaction mixture was cooled to 2 °C prior to the reaction commencing upon stirring (1200 rpm). The reaction was allowed to proceed for 0.5 h, after which, the catalyst was removed from the reaction solvents via filtration, and as described previously, two aliquots of 0.05 g were titrated against the acidified Ce(SO₄)₂ solution using ferroin as an indicator. Catalyst degradation activity is reported as mol_{H₂O₂} kg_{cat}⁻¹ h⁻¹.

Ketone Ammoximation via the In Situ Synthesis of H₂O₂. Catalysts were evaluated for their activity toward ketone ammoximation with the procedure for cyclohexanone ammoximation outlined below using a stainless-steel autoclave (Parr Instruments) with a nominal volume of 100 mL, equipped with a PTFE liner and a maximum working pressure of 2000 psi.

The autoclave was charged with the catalyst (0.075 g), solvent [H₂O (7.5 g, HPLC grade, Fisher Scientific) and *t*-BuOH (5.9 g, Merck)], cyclohexanone (0.196 g, 2.0 mmol, Merck), and ammonium bicarbonate (0.32 g, 4.0 mmol, Merck). *t*-BuOH was chosen as co-solvent due to the enhanced solubility of H₂, in comparison to H₂O, and the ability of *t*-BuOH to aid in the maintenance of the -Ti-O-Si- moiety, known to be responsible for the high activity of TS-1.²⁹ The reactor was purged three times with 5% H₂/N₂ (100 psi) and then filled with 5% H₂/N₂ (420 psi) and 25% O₂/N₂ (160 psi) to give a H₂:O₂ ratio of 1:2. All pressures are provided as gauge pressures, and reactant gases were not continuously introduced into the reactor. The reactor was stirred (100 rpm), while the reaction temperature was raised to 80 °C at which time stirring was increased to 800 rpm. The reaction was allowed to run for 6 h, unless otherwise stated, after which the reactor was cooled to 25 °C while stirring (100 rpm), using ice water. The reactant gas was collected for analysis gas chromatography using a Varian CP-3380 equipped with a TCD and a Porapak Q column. To the reaction solution, EtOH (6 g, HPLC grade, Fischer Scientific) and diethylene glycol monoethyl ether (external standard, 0.15 g, Merck) were added, with the former used to ensure complete homogeneity of the post-reaction solution, while the latter was chosen as an external standard. Following this, the catalyst was removed by filtration and the resulting solution was analyzed by gas chromatography using a Varian 3800 equipped with FID and a CP-Wax 52 CB column.

For reactions conducted in the presence of H₂ or O₂ alone, the pressure of the reagent (5% H₂/N₂ or 25% O₂/N₂) was identical to that used in the in situ reaction, with total pressure maintained at 580 psi using N₂. For reactions using commercial H₂O₂ (50 wt %, Fischer Scientific), the concentration of H₂O₂ utilized was identical to that which may be generated if all the H₂ in the in situ reaction was converted to H₂O₂; in this case, the oxidant was added to the reaction mixture, prior to the start of the reaction, and replaced part of the H₂O component; again, total pressure was maintained using N₂ (580 psi).

For reactions utilizing ketones other than cyclohexanone (cyclopentanone, cycloheptanone, cyclooctanone, and cyclododecanone), all chemicals were purchased from Merck. For calibration purposes, cyclohexanone oxime and cyclododecanone oxime were purchased from Merck. Cyclopentanone oxime and cyclooctanone oxime were purchased from Alfa Aesar, while cycloheptanone oxime was purchased from ChemCruz. All chemicals were used as received.

Ketone conversion and selectivity toward the oxime were calculated on the basis of starting amount of the ketone, according to eqs 1 and 2, respectively.

$$X_{\text{ketone}} = \frac{n_{\text{ketone}}(t(0)) - n_{\text{ketone}}(t(1))}{n_{\text{ketone}}(t(0))} \times 100 \quad (1)$$

$$S_{\text{oxime}} = \frac{n_{\text{oxime}}}{n_{\text{ketone}}(t(0)) - n_{\text{ketone}}(t(1))} \times 100 \quad (2)$$

Total autoclave capacity was determined via water displacement to allow for accurate determination of H₂ conversion and oxime selectivity based on H₂. When equipped with a PTFE liner (reducing nominal volume to 66 mL), the total volume of an unfilled autoclave was determined to be 93 mL, which includes all available gaseous space within the autoclave.

H₂ conversion and selectivity based on H₂ were calculated on the basis of starting amount of H₂ and the yield of oxime as determined from eqs 3 and 4.

$$X_{\text{H}_2} = \frac{n_{\text{H}_2(t(0))} - n_{\text{H}_2(t(1))}}{n_{\text{H}_2(t(0))}} \times 100 \quad (3)$$

$$S_{\text{H}_2} = \frac{n_{\text{oxime}}}{\left(\frac{n_{\text{H}_2(t(0))} - n_{\text{H}_2(t(1))}}{n_{\text{H}_2(t(0))}} \right)} \times 100 \quad (4)$$

Time-on-Line Analysis for Ketone Ammoximation via the In Situ Synthesis of H₂O₂. An identical procedure to that outlined above for ketone ammoximation via the in situ production of H₂O₂ is followed for the desired reaction time. It should be noted that individual experiments were carried out and the reaction mixture was not sampled on-line.

Hot-Filtration Experiments for Ketone Ammoximation via the In Situ Synthesis of H₂O₂. Catalytic activity is determined in a similar manner to that outlined above for ketone ammoximation using a 0.66%PdAu/TS-1 catalyst (0.075 g). After a 1.5 h reaction, the solid catalyst was removed by filtration from the reaction solution and replaced with bare TS-1 (0.075 g, HighChem), with the reaction solution returned to the autoclave. The reactor was then recharged with reagent gases (5%H₂/N₂ (420 psi) and 25%O₂/N₂ (160 psi) and allowed to proceed for a further 1.5 h, as described above. In this case, the bare TS-1 was used as received.

Catalyst Reusability in the Ammoximation of Ketones via the In Situ Synthesis of H₂O₂. In order to determine catalyst reusability, a similar procedure to that outlined above for ketone ammoximation via the in situ production of H₂O₂ was followed utilizing 0.3 g of catalyst. Following the initial test, the catalyst was recovered by filtration, washed with EtOH (6 g, Fischer Scientific), and dried (30 °C, 17 h, under vacuum). Next, 0.075 g of material from the recovered catalyst sample was used to conduct a standard ammoximation experiment.

Catalyst Characterization. Investigation of the bulk structure of the crystalline materials was carried out using a (θ - θ) PANalytical X'pert Pro powder diffractometer using a Cu K α radiation source, operating at 40 keV and 40 mA. Standard analysis was carried out using a 40 min run with a back filled sample, between 2θ values of 10–80°. Phase identification was carried out using the International Centre for Diffraction Data.

Note 4: X-ray diffractograms of key as-prepared catalysts are reported in Figure S1, with no reflections associated with active metals, indicative of the relatively low total loading of the immobilized metals.

X-ray photoelectron spectroscopy (XPS) analyses were made on a Kratos Axis Ultra DLD spectrometer. Samples were mounted using double-sided adhesive tape, and binding energies were referenced to the C(1s) binding energy of adventitious carbon contamination taken to be 284.8 eV. Monochromatic AlK α radiation was used for all measurements; an analyzer pass energy of 160 eV was used for survey scans, while 40 eV was employed for detailed regional scans. The intensities of the Au(4f) and Pd(3d) features were used to derive the Au/Pd surface ratios and Ti(2p) and Si(2p) features used to derive the Si/Ti surface ratios. All data were processed using CasaXPS v2.3.24 using a Shirley background and

modified Wagner elemental sensitivity factors as supplied by the instrument manufacturer.

Note 5: Given the low metal loading of these materials and the propensity for analysis-induced reduction, the XP data were acquired in an optimized time frame to minimize such reduction but still with a workable signal-to-noise ratio.

Fourier-transform infrared spectroscopy (FTIR) was carried out with a Bruker Tensor 27 spectrometer fitted with a HgCdTe (MCT) detector and operated with OPUS software.

Diffuse reflectance infrared Fourier-transform spectroscopy (DRIFTS) measurements were taken on a Bruker Tensor 27 spectrometer fitted with an MCT detector. A sample was loaded into the Praying Mantis high-temperature (HVC-DRP-4) in situ cell before exposure to N₂ and then 1% CO/N₂ at a flow rate of 50 cm³ min⁻¹. A background spectrum was obtained using KBr, and measurements were recorded every 1 min at room temperature. Once the CO adsorption bands in the DRIFT spectra ceased to increase in size, the gas feed was changed back to N₂ and measurements were repeated until no change in subsequent spectra was observed.

Metal leaching was quantified via analysis of post-reaction solutions via inductively coupled plasma mass spectrometry (ICP-MS) using an Agilent 7900 ICP-MS equipped with an I-AS auto-sampler using a five-point calibration using certified reference materials from Perkin Elmer and certified internal standard from Agilent. All calibrants were matrix-matched.

Transmission electron microscopy (TEM) was performed on a JEOL JEM-2100 operating at 200 kV. Samples were prepared by dry deposition onto 300 mesh copper grids coated with holey carbon film.

Aberration corrected scanning transmission electron microscopy (AC-STEM) was performed using a probe-corrected Hitachi HF5000 S/TEM, operating at 200 kV. The instrument was equipped with bright field and high angle annular dark field (HAADF) detectors for high spatial resolution STEM imaging experiments. This microscope was also equipped with a secondary electron detector and dual Oxford Instruments X-ray energy-dispersive spectroscopy (X-EDS) detectors (2 × 100 mm²) having a total collection angle of 2.02 sr. Additional AC-STEM was performed using a ThermoFisher ThemisZ S/TEM, operating at 300 keV. The instrument was equipped with HAADF and a segmented DF4 detector for high spatial resolution for high spatial resolution STEM-HAADF and STEM-IDPC imaging experiments. The installed Super-X detector has a total area of 120 mm² and 0.7 sr solid angle. In situ measurements were also conducted using the Hitachi HF5000 instrument. The catalytic materials were heated from ambient temperature to 400 °C and analyzed by STEM-ADF and X-EDS to identify structural and compositional changes during oxidative heat treatment.

RESULTS AND DISCUSSION

Our initial investigations established the efficacy of a range of Pd-based, TS-1-supported, bimetallic catalysts, prepared by a wet co-impregnation procedure, toward the synthesis and subsequent degradation of H₂O₂ (Table S2). These experiments were carried out under reaction conditions, which have been previously reported to offer enhanced H₂O₂ stability (i.e., sub-ambient temperatures, an alcohol co-solvent, and a CO₂ gaseous diluent).²⁷ The limited activity of the bimetallic formulations toward H₂O₂ synthesis was clear, with the exception of the 0.33%Pd–0.33%Pt/TS-1 (38 mol_{H₂O₂}kg_{cat}⁻¹ h⁻¹) and 0.33%Pd–0.33%Au/TS-1 (44 mol_{H₂O₂}kg_{cat}⁻¹ h⁻¹)

formulations. Perhaps unexpectedly, given the extensive literature reporting the improved catalytic performance that can be achieved from the alloying of Pd with Au^{30–32} the H₂O₂ synthesis activity of the 0.66%Pd/TS-1 catalyst (66 mol_{H₂O₂}kg_{cat}⁻¹ h⁻¹) was found to be superior to the PdAu analogue, which may suggest a lack of the synergistic enhancement often reported for bimetallic PdAu catalysts.^{33,34} However, it should be noted that the rate of H₂O₂ synthesis over the 0.33%Pd–0.33%Au/TS-1 catalyst was far greater than that of the 0.33%Pd/TS-1 analogue (28 mol_{H₂O₂}kg_{cat}⁻¹ h⁻¹). When also considering the limited activity of the 0.33%Au/TS-1 catalyst (2 mol_{H₂O₂}kg_{cat}⁻¹ h⁻¹), it can be concluded that the observed activity of the bimetallic formulation is not cumulative and a synergistic enhancement does indeed result from the alloying of the two metals. Although it may be possible to consider such an improvement exists to a lesser extent than that previously reported for a range of supported PdAu catalysts.^{35,36}

In keeping with the poor performance of the majority of the bimetallic catalysts toward H₂O₂ production, activity toward the in situ ammoxidation of cyclohexanone to the oxime was also found to be limited, again with the exception of the 0.33% Pd–0.33%Pt/TS-1 (69% oxime yield) and 0.33%Pd–0.33% Au/TS-1 (95% oxime yield) formulations (Figure 1). The

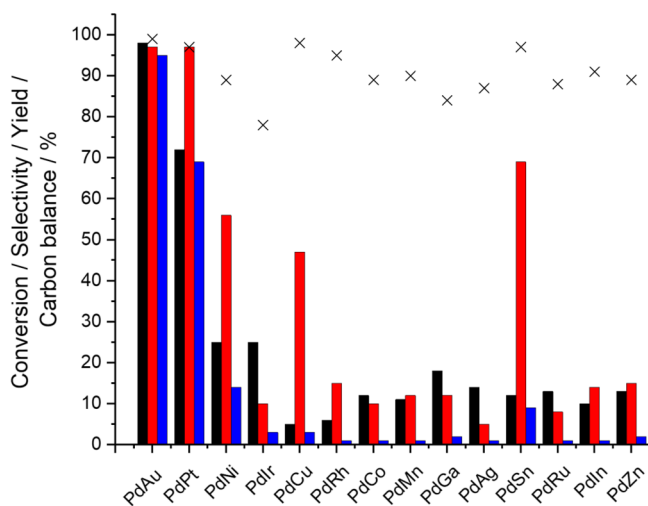


Figure 1. Catalytic activity of TS-1-supported Pd-based catalysts toward the ammoxidation of cyclohexanone via the in-situ synthesis of H₂O₂. Ammoxidation reaction conditions: Ketone (2 mmol), NH₄HCO₃ (4 mmol), 5% H₂/N₂ (4.7 mmol), 25% O₂/N₂ (6.1 mmol), catalyst (0.075 g), *t*-BuOH (5.9 g), H₂O (7.5 g), 6 h, 80 °C 800 rpm. Key: Cyclohexanone conversion (black bars), oxime selectivity (red bars), oxime yield (blue bars), and carbon balance (crosses). Note 1: Total metal loading is 0.66 wt % with Pd; X ratio = 1: 1 (wt/wt). Note 2: All catalysts were exposed to an oxidative heat treatment prior to testing (static air, 400 °C, 3 h, 10 °Cmin⁻¹).

considerable enhancement in cyclohexanone ammoxidation activity in the presence of a combination of H₂ and O₂ compared to that observed when using either reagent alone should also be noted (Figure S2). Extending this study further also revealed that synthesizing H₂O₂ in situ led to an increase in cyclohexanone oxime production compared to that observed when using commercially available H₂O₂ (70% oxime yield), at a concentration comparable to that present if all the H₂ present in the in situ reaction was selectively converted to the oxidant. The lower reactivity observed when utilizing the preformed

oxidant can be attributed to the complete addition of H₂O₂ prior to the reaction commencing. Indeed, for industrial application, the continual addition of H₂O₂ is well known to dictate catalytic performance.³⁷

The synergy resulting from the alloying of Pd and Au has been extensively studied for the direct synthesis of H₂O₂^{30,38–40} and a range of selective oxidative transformations (using O₂^{41,42} and H₂O₂^{43,44}), with similar observations made within this work for H₂O₂ direct synthesis (Table S2). Likewise, the activity of the bimetallic 0.33%Pd–0.33%Au/TS-1 catalyst toward cyclohexanone ammoxidation was also found to greatly exceed that observed over the 0.66%Au/TS-1 (2% oxime yield) or 0.66%Pd/TS-1 (10% oxime yield) analogues (Figure 2), with the enhanced activity of the

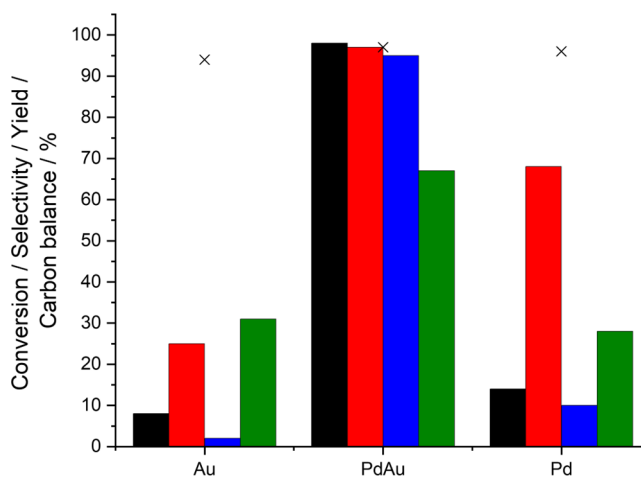


Figure 2. Effect of alloying Au and Pd on catalytic activity toward the ammoxidation of cyclohexanone via in situ H₂O₂ production. Key: Cyclohexanone conversion (black bars), oxime selectivity (red bars), oxime yield (blue bars), H₂ selectivity (green bars), and carbon balance (crosses). Ammoxidation reaction conditions: Cyclohexanone (2 mmol), NH₄HCO₃ (4 mmol), 5% H₂/N₂ (420 psi), 25% O₂/N₂ (160 psi), catalyst (0.075 g), *t*-BuOH (5.9 g), H₂O (7.5 g), 6 h, 80 °C, 800 rpm. Note: Au refers to 0.66%Au/TS-1, Pd to 0.66%Pd/TS-1 and PdAu to 0.33%Pd–0.33%Au/TS-1.

bimetallic formulation further highlighted through comparison of catalytic performance as a function of reaction time (Table S3) and determination of apparent reaction rate (Table S4). Importantly, we further observed that when the in situ ammoxidation reaction was not limited by cyclohexanone availability (20% cyclohexanone conversion at 1.5 h over the 0.33%Pd–0.33%Au/TS-1 catalyst), relatively high selective utilization of H₂ (i.e., the mols of H₂ selectively utilized in the formation of the oxime) could be achieved (84% H₂ selectivity). This metric was found to decrease as the reaction proceeds and the availability of cyclohexanone becomes limited (Table S3) and can be considered to be associated with the increased nonselective consumption of H₂ through H₂O₂ degradation pathways.

The synergistic enhancement observed through the formation of PdAu alloys has been typically attributed to a combination of the disruption of contiguous Pd ensembles and electronic modification, with Au acting as a promoter for Pd.^{45–47} Indeed, numerous studies have demonstrated that the introduction of Au into Pd surfaces not only inhibits the cleavage of O–O bonds (in *O₂, *OOH, or *H₂O₂ species), and the resulting formation of H₂O, but also promotes the

release of surface-bound H_2O_2 .^{38,48} These earlier works coupled with the enhanced performance and selectivity of the 0.33%Pd–0.33%Au/TS-1 catalyst suggests that the presence of Au is likely key in facilitating the desorption of H_2O_2 from PdAu surfaces, which subsequently diffuses to Ti^{IV} sites present within the TS-1 framework, where it is utilized in hydroxylamine formation. With the crucial role of Au established, we next investigated the effect of Pd: Au ratio on catalytic performance, while maintaining total metal loading at 0.66 wt %. In keeping with our previous studies into PdAu nanoparticles supported on TS-1²⁸ and SiO_2 ,⁴⁹ as well as our investigations within this work (Table S2), catalytic activity toward both the direct synthesis and subsequent degradation of H_2O_2 was found to correlate well with total Pd content. Indeed, the 0.66%Pd/TS-1 catalyst offered a greater activity toward both the direct synthesis of H_2O_2 ($66 \text{ mol}_{\text{H}_2\text{O}_2}\text{kg}_{\text{cat}}^{-1} \text{ h}^{-1}$), as well as its subsequent degradation ($209 \text{ mol}_{\text{H}_2\text{O}_2}\text{kg}_{\text{cat}}^{-1} \text{ h}^{-1}$), in comparison to the Au-only or bimetallic analogues (Table S5).

Evaluation of the performance of the TS-1 supported catalysts toward cyclohexanone ammoxidation identified an optimal nominal composition of 0.33%Pd–0.33%Au/TS-1, with this catalyst greatly outperforming either Au-rich or Pd-rich compositions (Figure 3, comparison of apparent rates of

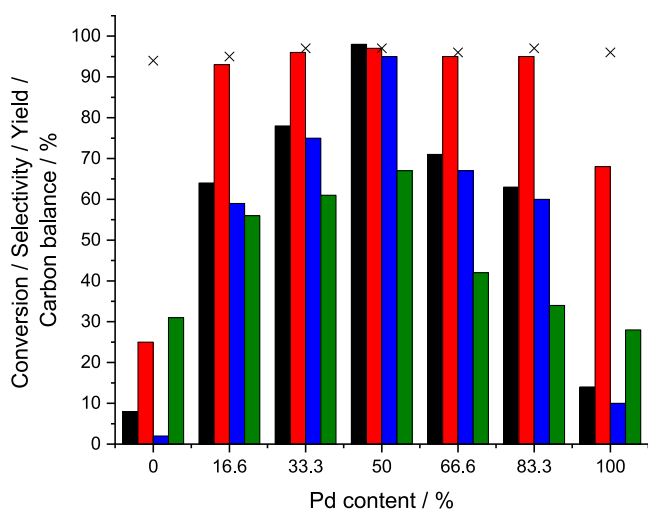


Figure 3. Effect of Pd:Au ratio on the catalytic activity of 0.66% PdAu/TS-1 catalysts toward the ammoxidation of cyclohexanone via the in situ production of H_2O_2 . Key: Cyclohexanone conversion (black bars), oxime selectivity (red bars), oxime yield (blue bars), H_2 selectivity (green bars), and carbon balance (crosses). Ammoxidation reaction conditions: Cyclohexanone (2 mmol), NH_4HCO_3 (4 mmol), 5% H_2/N_2 (420 psi), 25% O_2/N_2 (160 psi), catalyst (0.075 g), *t*-BuOH (5.9 g), H_2O (7.5 g), 6 h, 80 °C, 800 rpm.

reaction shown in Table S6), with the enhanced activity of all PdAu catalysts compared to monometallic analogues further highlighting the role of alloy formation in achieving enhanced catalytic performance. The relationship between catalytic activity toward the direct synthesis (and degradation) of H_2O_2 and the in situ ammoxidation of cyclohexanone was subsequently compared (Figure S3), with such observations highlighting the need for future catalyst development to focus both on improving activity toward H_2O_2 production and minimizing competitive H_2O_2 degradation pathways.

The catalytic performance of Pd-based catalysts toward H_2O_2 is known to be highly dependent on Pd oxidation state,

with a range of studies demonstrating the enhanced efficacy of Pd^{2+} – Pd^0 domains toward H_2O_2 production in comparison to Pd^{2+} or Pd^0 counterparts.^{46,50} An analysis of the supported PdAu catalysts via XPS indicates an increase in Pd^0 content with the introduction of Au (Figure S.4). Such observations suggest that, at least in part, the modification of Pd speciation through alloying with Au may be key to achieving high catalytic efficacy. However, it should be noted that such analysis is not representative of metal speciation in situ.

With our analysis by XPS demonstrating that the formation of PdAu alloys results in a considerable modification in Pd speciation (Figure S4), we were subsequently motivated to probe this catalytic series via CO-DRIFTS (Figure S5). The DRIFTS spectra of all catalysts were found to be dominated by Pd–CO bands, with the exception of the Au-rich formulations (0.66%Au/TS-1 and 0.11%Pd–0.55%Au/TS-1), where a combination of low (or no) Pd content and the transient nature of the Au–CO interaction at ambient temperature is considered the cause for the lack of an observable signal for these formulations.³⁰ It is possible to attribute the peaks within the higher wavenumber region of the spectra (approx. 2200–2000 cm^{-1}) to CO linearly adsorbed to low coordination Pd sites (i.e., edges or corners), while those centered at lower wavenumbers (2000–1800 cm^{-1}) can be assigned to the multifold adsorption of CO on extended Pd domains (i.e., species adsorbed in a bidentate or tridentate manner). A blueshift was found to result from the formation of PdAu nanoalloys, which is in keeping with observations made by Wilson et al.⁵¹ and can be attributed to the resulting charge transfer between Au and Pd.⁵² As such, based on our combined XPS and CO-DRIFTS analysis, it is possible to conclude that the improved reactivity of the PdAu/TS-1 catalyst, in part, can be related to the electronic modification of Pd through the formation of alloy structures.

Focusing on the optimal 0.33%Pd–0.33%Au/TS-1 formulation, we subsequently broadened our investigation to determine the effect of calcination temperature on catalytic performance. Analysis by FTIR (Figure S6, Supplementary Note 1) reveals no clear change in the observed positions of absorption bands compared to those identified through analysis of the as-supplied support material, over the temperature range studied (85–400 °C), suggesting that the structure of TS-1 remains unchanged during immobilization of precious metals and subsequent calcination, which is in keeping with the known high thermal stability of TS-1.⁵³ Further analysis by XRD (Figure S7, Supplementary Note 2) corroborates these observations. Notably, no reflections associated with precious metals were observed, which may be expected given the low total metal loading of these materials.

A strong correlation between calcination temperature and catalytic activity toward H_2O_2 synthesis, under conditions optimized for H_2O_2 production, was observed (Table S7), with the need to expose the catalyst to a minimum temperature of 400 °C (3 h, static air) to ensure stability under H_2O_2 direct synthesis conditions (Table S8). Despite displaying the greatest activity toward H_2O_2 synthesis ($80 \text{ mol}_{\text{H}_2\text{O}_2}\text{kg}_{\text{cat}}^{-1} \text{ h}^{-1}$), the performance of the dried-only catalyst (85 °C, 16 h, static air) toward the in situ ammoxidation of cyclohexanone was found to be extremely limited (6% oxime yield) (Figure 4). However, upon exposure to an elevated oxidative treatment, cyclohexanone oxime yield increased considerably (95% oxime yield after exposure to calcination at 400 °C).

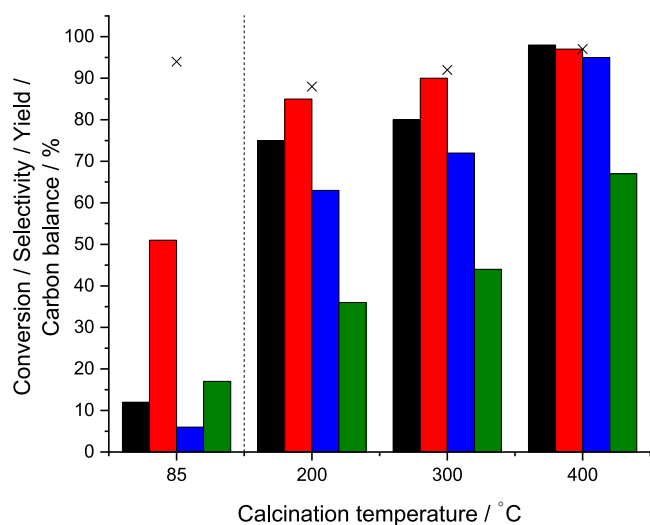


Figure 4. Effect of calcination temperature on catalytic performance of the 0.33%Pd–0.33%Au/TS-1 catalyst toward the ammoxidation of cyclohexanone via the in situ production of H₂O₂. Key: Cyclohexanone conversion (black bars), oxime selectivity (red bars), oxime yield (blue bars), H₂ selectivity (green bars), and carbon balance (crosses). Ammoxidation reaction conditions: Cyclohexanone (2 mmol), NH₄HCO₃ (4 mmol), 5% H₂/N₂ (420 psi), 25% O₂/N₂ (160 psi), catalyst (0.075 g), *t*-BuOH (5.9 g), H₂O (7.5 g), 6 h, 80 °C, 800 rpm.

Notably, a significant improvement in selective H₂ utilization was also found to coincide with exposure to increasing calcination temperature. XPS analysis of this subset of materials (Figure S8, Supplementary Note 3) indicated a stark shift in Pd: Au ratio and the formation of PdO as a result of high-temperature calcination, which may be indicative of nanoparticle agglomeration and Pd surface migration during calcination.⁵⁴

Determination of catalyst stability through ICP-MS analysis of post-reaction solutions revealed considerable leaching of Pd after use in the cyclohexanone ammoxidation reaction (Table S9), particularly for the dried-only catalyst, with this metric decreasing upon exposure to a high-temperature oxidative treatment. The leaching of Au was considerably less and decreased to zero with exposure to calcination temperatures of greater than 300 °C. Such observations are in keeping with earlier investigations into supported PdAu catalysts for numerous chemical transformations,⁵⁵ including H₂O₂ direct synthesis,⁵⁶ with the improved stability which results from high-temperature calcination attributed to enhanced metal-support interactions.^{36,57} It should be noted that we have recently demonstrated the improved stability of PdAu alloys, when compared to Pd-only species, during the in situ

ammoxidation of cyclohexanone, and identified that it is the ammonia reagent which is primarily responsible for the observed leaching of Pd.²³ As such, it is possible that the observed decrease in Pd leaching as a result of oxidative thermal treatment is indicative of the formation of bimetallic alloys.

TEM analysis of the 0.33%Pd–0.33%Au/TS-1 catalyst indicated the limited immobilization of the active metal species onto the majority TS-1 component (Figure S9), with further HAADF-STEM analysis highlighting the preferential deposition onto the minority TiO₂ component (Figure S10). A degree of variation in mean particle size was observed, regardless of the calcination temperature employed (Table 1). However, based on TEM analysis, a major proportion of metal nanoparticles in all samples were found to be below 10 nm, with a number of very large particles (>20 nm) also detected, which is typical of the wet impregnation route to catalyst preparation.^{58,59} Our TEM analysis also revealed a shift in mean nanoparticle size upon calcination at elevated temperatures, with this metric increasing from 3.8 nm for the dried-only material to 6.6 nm for the analogous catalyst exposed to a calcination temperature of 400 °C, although it is again worth highlighting that a significant proportion of the smaller (<10 nm) immobilized species are retained despite exposure to high-temperature calcination.

Analysis of the dried only (85 °C, 16 h) 0.33%Pd–0.33%Au/TS-1 catalyst by X-EDS revealed that the immobilized metal species existed as large Au-only nanoparticles, Au-rich alloys, or sub-nano Pd-only clusters, notably no Pd-only nanoparticles were detected (Figures S.11–13). Upon exposure to calcination temperatures exceeding 200 °C, it was possible to observe the agglomeration of metal species (Figure 5, with further data reported in Figures S.14 and 15), which aligns with our TEM (Table 1) and XPS (Figure S8, Supplementary Note 3) analysis. A clear shift in nanoparticle composition was also detected, with the incorporation of Pd into the larger Au-rich nanoparticles (Figures S.14). The formation of Pd-only nanoparticles was also observed, which can be attributed to the agglomeration of the Pd clusters identified in the dried only material. Such analysis, in addition to our earlier studies, which revealed the limited activity of monometallic Au and Pd catalysts (Figure 2) and that of the dried-only 0.33%Pd–0.33%Au/TS-1 catalyst, (Figure 4) indicates that the presence of PdAu alloy species is largely responsible for the observed reactivity toward cyclohexanone ammoxidation. However, the minor contribution from elementally segregated species should not be disregarded.

Detailed analysis of the fresh 0.33%Pd–0.33%Au/TS-1 catalyst (calcined at 400 °C) by HAADF-STEM and X-EDS elemental mapping (Figure 6, with additional data reported in

Table 1. Effect of Calcination Temperature on the Mean Particle Size of the 0.33%Pd–0.33%Au/TS-1 Catalyst, as Determined by TEM

calcination temperature/°C	mean particle size/nm (S.D.)	productivity/mol _{H₂O₂} kg _{cat} ⁻¹ h ^{-1a}	oxime yield/% ^b
dried only	3.8 (2.5)	80	6
200	3.8 (3.9)	62	63
300	6.2 (5.6)	53	72
400	6.6 (9.1)	44	95

^aH₂O₂ direct synthesis reaction conditions: Catalyst (0.01 g), H₂O (2.9 g), MeOH (5.6 g), 5% H₂/CO₂ (420 psi), 25% O₂/CO₂ (160 psi), 0.5 h, 2 °C 1200 rpm. ^bAmmoxidation reaction conditions: Cyclohexanone (2 mmol), NH₄HCO₃ (4 mmol), 5% H₂/N₂ (4.7 mmol), 25% O₂/N₂ (6.1 mmol), catalyst (0.075 g), *t*-BuOH (5.9 g), H₂O (7.5 g), 6 h, 80 °C, 800 rpm. Note: The dried only catalyst was treated at 85 °C, 16 h, static air.

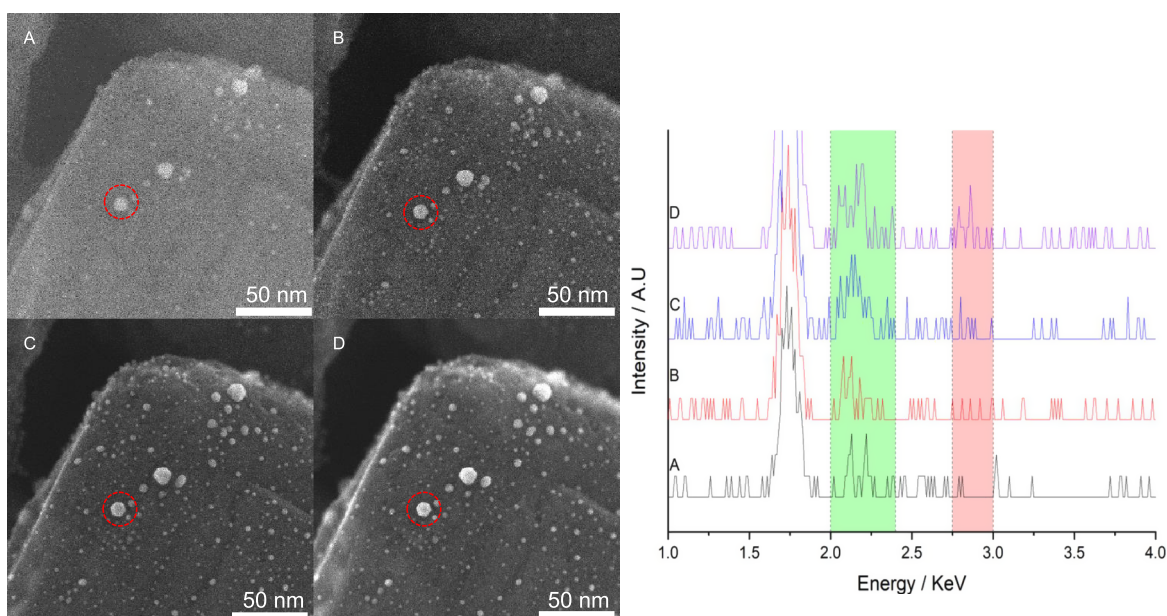


Figure 5. In situ secondary electron (SE in STEM) imaging and corresponding X-EDS analysis (Au ($M\alpha$) and Pd ($L\alpha$) centered at 2.12 and 2.84 keV respectively) of the indicated nanoparticle demonstrating the formation of PdAu alloys as a result of exposure of the 0.33%Pd–0.33%Au/TS-1 catalyst to an oxidative thermal treatment. (A) Dried-only, (B) 200 °C, (C) 300 °C, and (D) 400 °C. Note: the dried only sample was exposed to 85 °C, static air, 16 h. Conditions for calcination: static air, 3 h, 10 °C min^{-1} .

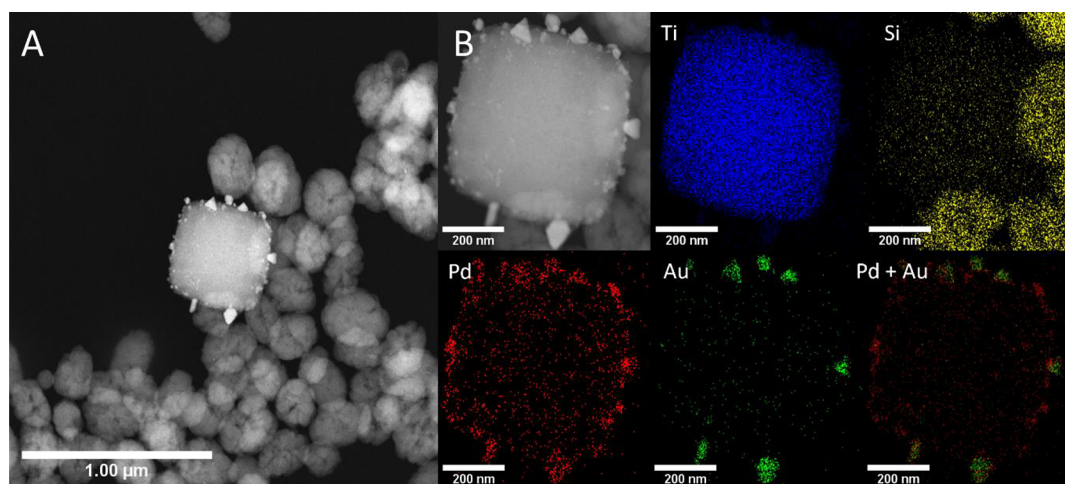


Figure 6. Microstructural analysis of the 0.33%Pd–0.33%Au/TS-1 catalyst including (A) HAADF-STEM image showing the preferential deposition of precious metal nanoparticles onto the TiO_2 minority component and (B) HAADF-STEM image and X-EDS mapping of the highlighted area showing the presence of PdAu alloys and smaller Pd nanoparticles, Au (green), Pd (red), Ti (blue), and Si (yellow).

Figures S.16 and 17) supported our in situ analysis (Figure 5) and identified the presence of both Pd-only nanoparticles and PdAu nanoalloys. A bimodal particle size distribution and a distinctive relationship between particle size and elemental composition has been typically reported for PdAu catalysts prepared by the wet co-impregnation route to catalyst synthesis, where larger particles are found to be Au-rich, PdAu alloys, and the smaller nanoparticles consist of Pd only.^{54,59} Similar observations can be made in this work; however, it is clear from our in situ STEM analysis (Figure 5) that the PdAu nanoalloys exist over a large particle size range, whereas no large (>20 nm) Pd-only species were observed.

With the leaching of metal species during use in the in situ ammoxidation reaction established (Table S9) and with a particular focus on the 0.33%Pd–0.33%Au/TS-1 catalyst exposed to a high-temperature oxidative heat treatment (400

°C), we next investigated catalyst stability upon reuse (Figure S18) and determined that there was no loss in reactivity, despite the observed loss of Pd. Investigation of the used 0.33%Pd–0.33%Au/TS-1 catalyst by HAADF-STEM and X-EDS correlates well with our ICP-MS analysis and identified that the Pd leaching is associated with the loss of the unalloyed Pd species, whereas the PdAu nanoparticles were retained after use (Figure S19). We subsequently conducted a series of hot-filtration experiments to identify the contribution of homogeneous metal species to the observed reactivity (Figure 7A,B). In the absence of the heterogeneous catalyst, no additional cyclohexanone conversion was observed, with this metric identical to that during the initial 1.5 h reaction, which was conducted in the presence of the 0.33%Pd–0.33%Au/TS-1 catalyst (20% cyclohexanone conversion). To identify if the lack of activity observed during the two-part hot-filtration

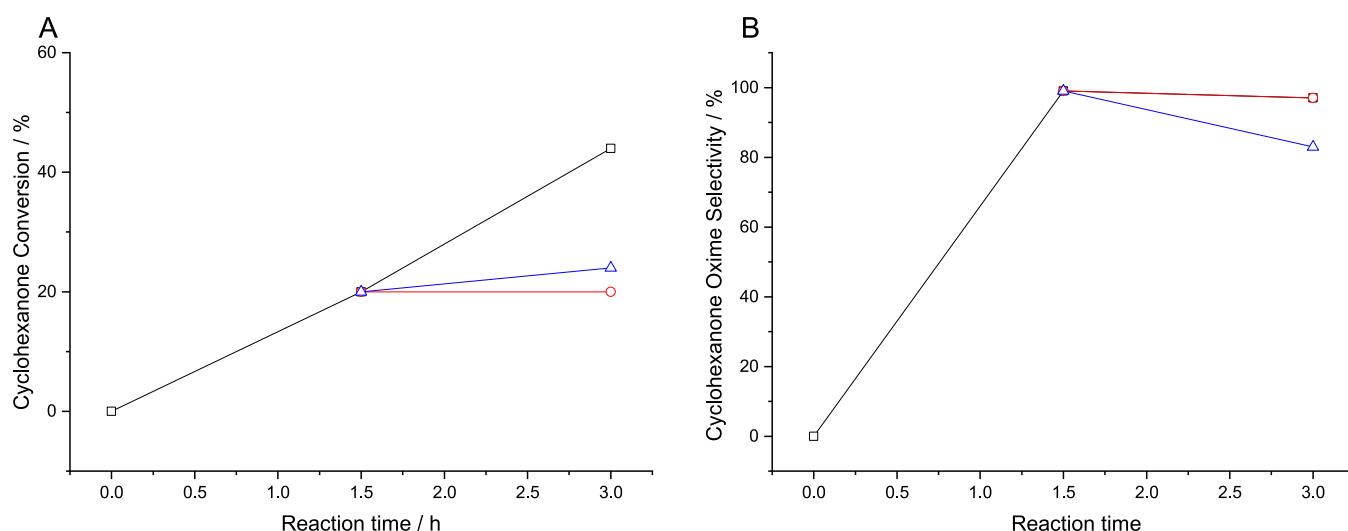


Figure 7. Efficacy of leached species in the ammoxidation of cyclohexanone as identified by a hot-filtration experiment using the 0.33%Pd–0.33% Au/TS-1 catalyst. (A) Cyclohexanone conversion and (B) cyclohexanone oxime selectivity. Key: Heterogeneously catalyzed reaction (black squares); hot-filtration reaction where the catalyst was removed by filtration prior to a final 1.5 h experiment (red circles); hot filtration where the catalyst was removed by filtration after 1.5 h and replaced by TS-1 for the final 1.5 h of reaction (blue triangles). Note 1: Catalyst exposed to an oxidative heat treatment (3 h, 400 °C, 10 °Cmin⁻¹, static air) prior to use. Note 2: In the case of the hot-filtration experiment where the heterogeneous 0.33%Pd–0.33%Au/TS-1 catalyst was replaced with TS-1 (0.075 g), the TS-1 catalyst was used as received. Ammoxidation reaction conditions: Cyclohexanone (2 mmol), NH₄HCO₃ (4 mmol), 5% H₂/N₂ (420 psi), 25% O₂/N₂ (160 psi), catalyst (0.075 g), *t*-BuOH (5.9 g), H₂O (7.5 g), reaction time 3 h, reaction temperature 80 °C, stirring speed 800 rpm.

experiment was due to the removal of the TS-1 component, a subsequent experiment was conducted, whereby after the initial 1.5 h, the heterogeneous catalyst was replaced with TS-1 (0.075 g), prior to replacing the gaseous reagents and recommencing the reaction for a further 1.5 h. Some additional conversion of cyclohexanone was detected (24% cyclohexanone conversion at 3 h). While this may be indicative of a homogeneous component to the reaction, it is notable that we did not observe any additional formation of cyclohexanone oxime. This in addition to the loss in selectivity to desired products in the second part of the hot-filtration experiment, and the known ability of TS-1 to catalyze unselective side reactions,⁶⁰ indicates that the contribution of any leached metal species toward cyclohexanone ammoxidation, if any, is negligible and that in the absence of the heterogeneous metal loaded catalyst the TS-1 component alone is responsible for the observed increase in cyclohexanone conversion.

Finally, again utilizing the optimal 0.33%Pd–0.33%Au/TS-1 catalyst, we broadened our studies to assess performance toward the in situ ammoxidation of a range of cyclic ketones (cyclopentanone, cycloheptanone, cyclooctenone, and cyclododecanone) (Figure 8), with many of the corresponding oximes having direct industrial application.^{61,62} Regardless of the substrate, selectivity toward the corresponding oxime was found to be high ($\geq 90\%$ in all cases). However, the extent of substrate conversion was found to differ over the series of ketones investigated. This is in keeping with previous studies utilizing commercial H₂O₂, with the variation in reactivity considered to result from the differing intrinsic reactivity of the ketones with the hydroxylamine intermediate, although diffusion limitations (i.e., the ability of the substrate to access the interior pore structure of the titanosilicate) should also be considered.⁶³

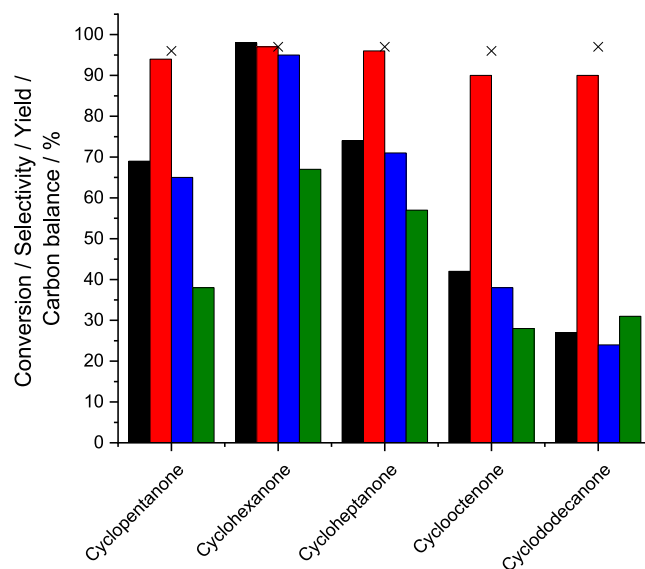


Figure 8. Catalytic activity of the 0.33%Au-0.33%Pd/TS-1 catalyst toward the ammoxidation of a range of ketones, via the in situ production of H₂O₂. Key: Ketone conversion (black bars), oxime selectivity (red bars), oxime yield (blue bars), H₂ selectivity (green bars), and carbon balance (crosses). Ammoxidation reaction conditions: Ketone (2 mmol), NH₄HCO₃ (4 mmol), 5% H₂/N₂ (420 psi), 25% O₂/N₂ (160 psi), catalyst (0.075 g), *t*-BuOH (5.9 g), H₂O (7.5 g), 6 h, 80 °C, 800 rpm.

CONCLUSIONS AND FUTURE PERSPECTIVES

The in situ synthesis of H₂O₂ over a bifunctional composite catalyst that is able to both synthesize H₂O₂ and subsequently utilize it in the formation of the hydroxylamine intermediate represents an attractive alternative to the current industrial route to the ammoxidation of cyclohexanone (and other ketones) to the corresponding oxime.

Within this work, we have demonstrated that using Pd-based nanoalloys supported on a commercially available TS-1, it is indeed possible to bridge the wide condition gap that exists between the individual reaction pathways (H_2O_2 synthesis and ketone ammoximation) and achieve selectivities and product yields approaching 100%. In particular, the alloying of Pd with Au was found to significantly improve catalytic activity. This is despite the higher H_2O_2 synthesis rates observed over the monometallic Pd catalyst and is attributed to the ability of Au to modify Pd speciation, inhibit competitive H_2O_2 degradation pathways (leading to enhanced H_2 utilization), and promote the release of the oxidant from metal surfaces for utilization by the TS-1 component. Notably, the formation of PdAu nanoalloys was also found to correlate with an improvement in catalyst stability.

It is considered that the in situ approach developed herein for ketone ammoximation has the potential to form the basis of an alternative route to numerous chemical transformations that currently utilize a combination of TS-1 and H_2O_2 , decoupling many industrial processes from large-scale, off-site H_2O_2 production. However, with a particular focus on the ammoximation of cyclohexanone, it is suggested that future studies be focused on the iterative development of both catalytically active sites, that is, the Ti^{IV} centers within the TS-1 component, responsible for hydroxylamine synthesis, and the metal species responsible for H_2O_2 production. There is still clearly a need for improvements in catalyst reactivity and selective H_2 utilization to be made, while diffusion limitations associated with the TS-1 pore structure should also be considered.

Furthermore, the loss of TS-1 crystallinity and formation of TiO_2 surface species is well known to result from the presence of ammonia in reactant streams and lead to catalyst deactivation during industrial use as well as promoting precious metal dissolution. While significant improvements in TS-1 stability have been made in recent years, there is a need to evaluate the long-term stability of immobilized metal species under real-world conditions and over extended time frames.

■ ASSOCIATED CONTENT

SI Supporting Information

The Supporting Information is available free of charge at <https://pubs.acs.org/doi/10.1021/acscatal.2c05799>.

Data relating to catalytic activity toward the direct synthesis and subsequent degradation of H_2O_2 and the in situ oxidation of cyclohexanone to the corresponding oxime, with accompanying characterization of catalytic materials via XRD, FTIR, XPS, CO-DRIFTS, TEM, HAADF-STEM, and X-EDS (PDF)

■ AUTHOR INFORMATION

Corresponding Authors

Richard J. Lewis – Max Planck–Cardiff Centre on the Fundamentals of Heterogeneous Catalysis FUNCAT, Cardiff Catalysis Institute, School of Chemistry, Cardiff University, Cardiff CF10 3AT, U.K.; orcid.org/0000-0001-9990-7064; Email: LewisR27@cardiff.ac.uk

Xi Liu – School of Chemistry and Chemical, In-situ Centre for Physical Sciences, Shanghai Jiao Tong University, 200240 Shanghai, P. R. China; Email: LiuXi@sjtu.edu.cn

Graham J. Hutchings – Max Planck–Cardiff Centre on the Fundamentals of Heterogeneous Catalysis FUNCAT, Cardiff

Catalysis Institute, School of Chemistry, Cardiff University, Cardiff CF10 3AT, U.K.; orcid.org/0000-0001-8885-1560; Email: Hutch@cardiff.ac.uk

Authors

Kenji Ueura – UBE Corporation, Yamaguchi 755-8633, Japan; orcid.org/0000-0002-2654-6955

Yukimasa Fukuta – UBE Corporation, Yamaguchi 755-8633, Japan

Tian Qin – School of Chemistry and Chemical, In-situ Centre for Physical Sciences, Shanghai Jiao Tong University, 200240 Shanghai, P. R. China; orcid.org/0000-0002-2856-4743

Thomas E. Davies – Max Planck–Cardiff Centre on the Fundamentals of Heterogeneous Catalysis FUNCAT, Cardiff Catalysis Institute, School of Chemistry, Cardiff University, Cardiff CF10 3AT, U.K.

David J. Morgan – Max Planck–Cardiff Centre on the Fundamentals of Heterogeneous Catalysis FUNCAT, Cardiff Catalysis Institute, School of Chemistry, Cardiff University, Cardiff CF10 3AT, U.K.; HarwellXPS, Research Complex at Harwell (RCaH), Didcot OX11 0FA, U.K.; orcid.org/0000-0002-6571-5731

Alex Stenner – Max Planck–Cardiff Centre on the Fundamentals of Heterogeneous Catalysis FUNCAT, Cardiff Catalysis Institute, School of Chemistry, Cardiff University, Cardiff CF10 3AT, U.K.

James Singleton – Max Planck–Cardiff Centre on the Fundamentals of Heterogeneous Catalysis FUNCAT, Cardiff Catalysis Institute, School of Chemistry, Cardiff University, Cardiff CF10 3AT, U.K.

Jennifer K. Edwards – Cardiff Catalysis Institute, School of Chemistry, Cardiff University, Cardiff CF10 3AT, U.K.

Simon J. Freakley – Department of Chemistry, University of Bath, Bath BA2 7AY, U.K.

Christopher J. Kiely – Department of Materials Science and Engineering, Lehigh University, Bethlehem, Pennsylvania 18015, United States

Liwei Chen – School of Chemistry and Chemical, In-situ Centre for Physical Sciences, Shanghai Jiao Tong University, 200240 Shanghai, P. R. China; School of Chemistry and Chemical, Frontiers Science Centre for Transformative Molecules, Shanghai 200240, P.R. China; orcid.org/0000-0003-4160-9771

Yasushi Yamamoto – UBE Corporation, Yamaguchi 755-8633, Japan

Complete contact information is available at: <https://pubs.acs.org/doi/10.1021/acscatal.2c05799>

Author Contributions

R.J.L., K.U., Y.F., S.J.F., and G.J.H. contributed to the design of the study; R.J.L. and K.U. conducted experiments and data analysis. R.J.L., K.U., X.L., Y.F., J.S., J.K.E., S.J.F., C.J.K., L.C., Y.Y., and G.J.H. provided technical advice and result interpretation. R.J.L., X.L., T.Q., T.E.D., D.J.M., A.S., and C.J.K. conducted catalyst characterization and corresponding data processing. R.J.L. wrote the manuscript and the supplementary material; all authors commented on and amended both documents. All authors discussed and contributed to the work.

Notes

The authors declare no competing financial interest.

ACKNOWLEDGMENTS

We appreciate technical support from Mr. Hiroaki Matsumoto and Mr. Chaobin Zeng, Hitachi High-Technologies (Shanghai) Co. Ltd., for HR-STEM characterization. The authors would like to thank the CCI-Electron Microscopy Facility, which has been funded partly by the European Regional Development Fund through the Welsh Government, and The Wolfson Foundation. XPS data collection was performed at the EPSRC National Facility for XPS (“HarwellXPS”), operated by Cardiff University and UCL, under contract No. PR16195. Funding: The authors thank UBE Corporation for financial support and technical advice, R.J.L., A.S and G.J.H gratefully acknowledge Cardiff University and the Max Planck Centre for Fundamental Heterogeneous Catalysis (FUNCAT) for financial support. X.L. acknowledges financial support from National Key R&D Program of China (2021YFA1500300) and National Natural Science Foundation of China (21872163 and 22072090). S.J.F. acknowledges the award of a Prize Research Fellowship from the University of Bath.

REFERENCES

- (1) Taramasso, M.; Perego, G.; Notari, B. Preparation of porous crystalline synthetic material comprised of silicon and titanium oxides, (Montedipe SpA). US 4410501A, 1983.
- (2) Puértolas, B.; Hill, A. K.; García, T.; Solsona, B.; Torrente-Murciano, L. In-situ synthesis of hydrogen peroxide in tandem with selective oxidation reactions: A mini-review. *Catal. Today* **2015**, *248*, 115–127.
- (3) Luo, Y.; Xiong, J.; Pang, C.; Li, G.; Hu, C. Direct Hydroxylation of Benzene to Phenol over TS-1 Catalysts. *Catalysts* **2018**, *8*, 49.
- (4) Schuster, W.; Niederer, J. P. M.; Hoelderich, W. F. The gas phase oxidative dehydrogenation of propane over TS-1. *Appl. Catal., A* **2001**, *209*, 131–143.
- (5) Aly, M.; Saeys, M. Selective silylation boosts propylene epoxidation with H₂ and O₂ over Au/TS-1. *Chem. Catal.* **2021**, *1*, 761–762.
- (6) Lin, M.; Xia, C.; Zhu, B.; Li, H.; Shu, X. Green and efficient epoxidation of propylene with hydrogen peroxide (HPPO process) catalyzed by hollow TS-1 zeolite: A 1.0 kt/a pilot-scale study. *Chem. Eng. J.* **2016**, *295*, 370.
- (7) Wang, G.; Du, W.; Duan, X.; Cao, Y.; Zhang, Z.; Xu, J.; Chen, W.; Qian, G.; Yuan, W.; Zhou, X.; Chen, D. Mechanism-guided elaboration of ternary Au–Ti–Si sites to boost propylene oxide formation. *Chem. Catal.* **2021**, *1*, 885–895.
- (8) Liu, G.; Wu, J.; Luo, H. Ammoxidation of Cyclohexanone to Cyclohexanone Oxime Catalyzed by Titanium Silicalite-1 Zeolite in Three-phase System. *Chin. J. Chem. Eng.* **2012**, *20*, 889.
- (9) HDIN Research, Global Nylon 6 Production Capacity reach to 8.86 million Tons in 2024 (2019) via <https://www.hdinresearch.com/news/56> (accessed July 21, 2022).
- (10) Chapman, S.; O'Malley, A. J.; Parker, S. F.; Raja, R. Comprehensive Vibrational Spectroscopic Characterization of Nylon-6 Precursors for Precise Tracking of the Beckmann Rearrangement. *ChemPhysChem* **2018**, *19*, 3196–3203.
- (11) Mokaya, R.; Poliakov, M. A Cleaner Way to Nylon? *Nature* **2005**, *437*, 1243–1244.
- (12) Mantegazza, M. A.; Cesana, A.; Pastori, M. Ammoxidation of ketones on titanium silicalite. A study of the reaction byproducts. *Top. Catal.* **1996**, *3*, 327–335.
- (13) Yip, A. C. K.; Hu, X. Catalytic Activity of Clay-Based Titanium Silicalite-1 Composite in Cyclohexanone Ammoxidation. *Ind. Eng. Chem. Res.* **2009**, *48*, 8441–8450.
- (14) Qi, Y.; Ye, C.; Zhuang, Z.; Xin, F. Preparation and evaluation of titanium silicalite-1 utilizing pretreated titanium dioxide as a titanium source. *Microporous Mesoporous Mater.* **2011**, *142*, 661–665.
- (15) Dal Pozzo, L.; Fornasari, G.; Monti, T. TS-1, catalytic mechanism in cyclohexanone oxime production. *Catal. Commun.* **2002**, *3*, 369.
- (16) Yip, A. C. K.; Hu, X. Formulation of Reaction Kinetics for Cyclohexanone Ammoxidation Catalyzed by a Clay-Based Titanium Silicalite-1 Composite in a Semibatch Process. *Ind. Eng. Chem. Res.* **2011**, *50*, 13703–13710.
- (17) Lewis, R. J.; Hutchings, G. J. Recent Advances in the Direct Synthesis of H₂O₂. *ChemCatChem* **2019**, *11*, 298.
- (18) Edwards, J. K.; Freakley, S. J.; Lewis, R. J.; Pritchard, J. C.; Hutchings, G. J. Advances in the direct synthesis of hydrogen peroxide from hydrogen and oxygen. *Catal. Today* **2015**, *248*, 3–9.
- (19) Campos-Martin, J. M.; Blanco-Brieva, G.; Fierro, J. L. G. Hydrogen Peroxide Synthesis: An Outlook beyond the Anthraquinone Process. *Angew. Chem., Int. Ed.* **2006**, *45*, 6962–6984.
- (20) Gao, G.; Tian, Y.; Gong, X.; Pan, Z.; Yang, K.; Zong, B. Advances in the production technology of hydrogen peroxide. *Chin. J. Catal.* **2020**, *41*, 1039–1047.
- (21) Liang, X.; Mi, Z.; Wang, Y.; Wang, L.; Zhang, X. Synthesis of acetone oxime through acetone ammoxidation over TS-1. *React. Kinet. Catal. Lett.* **2004**, *82*, 333–337.
- (22) Zajacek, J. G.; Crocco, G. L.; Jubin, J. C. Integrated process for cyclohexanone oxime production, (Lyondell Chemical Technology LP). EP 0690045A1, 1994
- (23) Lewis, R. J.; Ueura, K.; Liu, X.; Fukuta, Y.; Davies, T. E.; Morgan, D. J.; Chen, L.; Qi, J.; Singleton, J.; Edwards, J. K.; Freakley, S. J.; Kiely, C. J.; Yamamoto, Y.; Hutchings, G. J. Highly efficient catalytic production of oximes from ketones using in situ-generated H₂O₂. *Science* **2022**, *376*, 615–620.
- (24) Gallina, G.; García-Serna, J.; Salmi, T. O.; Canu, P.; Biasi, P. Bromide and Acids: A Comprehensive Study on Their Role on the Hydrogen Peroxide Direct Synthesis. *Ind. Eng. Chem. Res.* **2017**, *56*, 13367.
- (25) Liu, Q.; Gath, K. K.; Bauer, J. C.; Schaak, R. E.; Lunsford, J. H. The Active Phase in the Direct Synthesis of H₂O₂ from H₂ and O₂ over Pd/SiO₂ Catalyst in a H₂SO₄/Ethanol System. *Catal. Lett.* **2009**, *132*, 342.
- (26) Liu, Q.; Bauer, J. C.; Schaak, R. E.; Lunsford, J. H. Direct synthesis of H₂O₂ from H₂ and O₂ over Pd–Pt/SiO₂ bimetallic catalysts in a H₂SO₄/ethanol system. *Appl. Catal., A* **2008**, *339*, 130.
- (27) Santos, A.; Lewis, R. J.; Malta, G.; Howe, A. G. R.; Morgan, D. J.; Hampton, E.; Gaskin, P.; Hutchings, G. J. Direct Synthesis of Hydrogen Peroxide over Au–Pd Supported Nanoparticles under Ambient Conditions. *Ind. Eng. Chem. Res.* **2019**, *58*, 12623–12631.
- (28) Lewis, R. J.; Ueura, K.; Fukuta, Y.; Freakley, S. J.; Kang, L.; Wang, R.; He, Q.; Edwards, J. K.; Morgan, D. J.; Yamamoto, Y.; Hutchings, G. J. The Direct Synthesis of H₂O₂ Using TS-1 Supported Catalysts. *ChemCatChem* **2019**, *11*, 1673–1680.
- (29) Wu, C.; Wang, Y.; Mi, Z.; Xue, L.; Wu, W.; Min, E.; Han, S.; He, F.; Fu, S. Effects of organic solvents on the structure stability of TS-1 for the ammoxidation of cyclohexanone. *React. Kinet. Catal. Lett.* **2002**, *77*, 73–81.
- (30) Wilson, N. M.; Priyadarshini, P.; Kunz, S.; Flaherty, D. W. Direct synthesis of H₂O₂ on Pd and Au_xPd₁ clusters: Understanding the effects of alloying Pd with Au. *J. Catal.* **2018**, *357*, 163.
- (31) Ntainjua, N. E.; Edwards, J. K.; Carley, A. F.; Lopez-Sanchez, J. A.; Moulijn, J. A.; Herzing, A. A.; Kiely, C. J.; Hutchings, G. J. The role of the support in achieving high selectivity in the direct formation of hydrogen peroxide. *Green Chem.* **2008**, *10*, 1162–1169.
- (32) Menegazzo, F.; Manzoli, M.; Signoreto, M.; Pinna, F.; Strukul, G. H₂O₂ direct synthesis under mild conditions on Pd–Au samples: Effect of the morphology and of the composition of the metallic phase. *Catal. Today* **2015**, *248*, 18–27.
- (33) Brehm, J.; Lewis, R. J.; Morgan, D. J.; Davies, T. E.; Hutchings, G. J. The Direct Synthesis of Hydrogen Peroxide over AuPd Nanoparticles: An Investigation into Metal Loading. *Catal. Lett.* **2022**, *152*, 254–262.
- (34) Kanungo, S.; van Haandel, L.; Hensen, E. J. M.; Schouten, J. C.; Neira d'Angelo, M. F. Direct synthesis of H₂O₂ in AuPd coated micro

channels: An in-situ X-Ray absorption spectroscopic study. *J. Catal.* **2019**, *370*, 200.

(35) Edwards, J. K.; Hutchings, G. J. Palladium and Gold–Palladium Catalysts for the Direct Synthesis of Hydrogen Peroxide. *Angew. Chem., Int. Ed.* **2008**, *47*, 9192.

(36) Lewis, R. J.; Ueura, K.; Fukuta, Y.; Davies, T. E.; Morgan, D. J.; Paris, C. B.; Singleton, J.; Edwards, J. K.; Freakley, S. J.; Yamamoto, Y.; Hutchings, G. J. Cyclohexanone ammoximation via in situ H₂O₂ production using TS-1 supported catalysts. *Green Chem.* **2022**, 9496.

(37) Zhao, S.; Xie, W.; Yang, J.; Liu, Y.; Zhang, Y.; Xu, B.; Jiang, J.; He, M.; Wu, P. An investigation into cyclohexanone ammoximation over Ti-MWW in a continuous slurry reactor. *Appl. Catal., A* **2011**, *394*, 1–8.

(38) Li, Z.; Gao, L.; Zhu, X.; Ma, W.; Feng, X.; Zhong, Q. Synergistic Enhancement over Au-Pd/TS-1 Bimetallic Catalysts for Propylene Epoxidation with H₂ and O₂. *ChemCatChem* **2019**, *11*, 5116–5123.

(39) Edwards, J. K.; Solsona, B.; Edwin Ntainjua, N.; Carley, A. F.; Herzing, A. A.; Kiely, C. J.; Hutchings, G. J. Switching Off Hydrogen Peroxide Hydrogenation in the Direct Synthesis Process. *Science* **2009**, *323*, 1037.

(40) Agarwal, N.; Thomas, L.; Nasrallah, A.; Sainna, M. A.; Freakley, S. J.; Edwards, J. K.; Catlow, C. R. A.; Hutchings, G. J.; Taylor, S. H.; Willock, D. J. The direct synthesis of hydrogen peroxide over Au and Pd nanoparticles: A DFT study. *Catal. Today* **2021**, *381*, 76–85.

(41) Kesavan, L.; Tiruvalam, R.; Rahim, M. H. A.; Bin Saiman, M. I.; Enache, D. I.; Jenkins, R. L.; Dimitratos, N.; Lopez-Sanchez, J. A.; Taylor, S. H.; Knight, D. W.; Kiely, C. J.; Hutchings, G. J. Solvent-free oxidation of primary carbon-hydrogen bonds in toluene using Au-Pd alloy nanoparticles. *Science* **2011**, *331*, 195–199.

(42) Chang, C.; Long, B.; Yang, X.; Li, J. Theoretical Studies on the Synergetic Effects of Au–Pd Bimetallic Catalysts in the Selective Oxidation of Methanol. *J. Phys. Chem. C* **2015**, *119*, 16072–16081.

(43) Crombie, C. M.; Lewis, R. J.; Taylor, R. L.; Morgan, D. J.; Davies, T. E.; Folli, A.; Murphy, D. M.; Edwards, J. K.; Qi, J.; Jiang, H.; Kiely, C. J.; Liu, X.; Skjøth-Rasmussen, M. S.; Hutchings, G. J. Enhanced Selective Oxidation of Benzyl Alcohol via In Situ H₂O₂ Production over Supported Pd-Based Catalysts. *ACS Catal.* **2021**, *11*, 2701–2714.

(44) Xu, G.; Yu, A.; Xu, Y.; Sun, C. Selective oxidation of methane to methanol using AuPd@ZIF-8. *Catal. Commun.* **2021**, *158*, No. 106338.

(45) Chen, M.; Kumar, D.; Yi, C. W.; Goodman, D. W. The Promotional Effect of Gold in Catalysis by Palladium-Gold. *Science* **2005**, *310*, 291.

(46) Gong, X.; Lewis, R. J.; Zhou, S.; Morgan, D. J.; Davies, T. E.; Liu, X.; Kiely, C. J.; Zong, B.; Hutchings, G. J. Enhanced catalyst selectivity in the direct synthesis of H₂O₂ through Pt incorporation into TiO₂ supported AuPd catalysts. *Catal. Sci. Technol.* **2020**, *10*, 4635.

(47) Ricciardulli, T.; Gorthy, S.; Adams, J. S.; Thompson, C.; Karim, A. M.; Neurock, M.; Flaherty, D. W. Effect of Pd Coordination and Isolation on the Catalytic Reduction of O₂ to H₂O₂ over PdAu Bimetallic Nanoparticles. *J. Am. Chem. Soc.* **2021**, *143*, 5445–5464.

(48) Yao, Z.; Zhao, J.; Bunting, R. J.; Zhao, C.; Hu, P.; Wang, J. Quantitative Insights into the Reaction Mechanism for the Direct Synthesis of H₂O₂ over Transition Metals: Coverage-Dependent Microkinetic Modeling. *ACS Catal.* **2021**, *11*, 1202–1221.

(49) Edwards, J. K.; Parker, S. F.; Pritchard, J.; Piccinini, M.; Freakley, S. J.; He, Q.; Carley, A. F.; Kiely, C. J.; Hutchings, G. J. Effect of acid pre-treatment on AuPd/SiO₂ catalysts for the direct synthesis of hydrogen peroxide. *Catal. Sci. Technol.* **2013**, *3*, 812–818.

(50) Ouyang, L.; Tian, P.; Da, G.; Xu, X.; Ao, C.; Chen, T.; Si, R.; Xu, J.; Han, Y. The origin of active sites for direct synthesis of H₂O₂ on Pd/TiO₂ catalysts: Interfaces of Pd and PdO domains. *J. Catal.* **2015**, *321*, 70.

(51) Wilson, A. R.; Sun, K.; Chi, M.; White, R. M.; LeBeau, J. M.; Lamb, H. H.; Wiley, B. J. From Core–Shell to Alloys: The

Preparation and Characterization of Solution-Synthesized AuPd Nanoparticle Catalysts. *J. Phys. Chem. C* **2013**, *117*, 17557–17566.

(52) Han, Y.; Zhong, Z.; Ramesh, K.; Chen, F.; Chen, L.; White, T.; Tay, Q.; Yaakub, S. N.; Wang, Z. Au Promotional Effects on the Synthesis of H₂O₂ Directly from H₂ and O₂ on Supported Pd–Au Alloy Catalysts. *J. Phys. Chem. C* **2007**, *111*, 8410–8413.

(53) Drago, R. S.; Dias, S. C.; McGilvray, J. M.; Mateus, A. L. M. L. Acidity and Hydrophobicity of TS-1. *J. Phys. Chem. B.* **1998**, *102*, 1508–1514.

(54) Herzing, A. A.; Watanabe, M.; Edwards, J. K.; Conte, M.; Tang, Z. R.; Hutchings, G. J.; Kiely, C. J. Energy dispersive X-ray spectroscopy of bimetallic nanoparticles in an aberration corrected scanning transmission electron microscope. *Faraday Discuss.* **2008**, *138*, 337.

(55) Sasirekha, N.; Sangeetha, P.; Chen, Y.-W. Bimetallic Au–Ag/CeO₂ Catalysts for Preferential Oxidation of CO in Hydrogen-Rich Stream: Effect of Calcination Temperature. *J. Phys. Chem. C* **2014**, *118*, 15226–15233.

(56) Edwards, J. K.; Solsona, B. E.; Landon, P.; Carley, A. F.; Herzing, A.; Kiely, C. J.; Hutchings, G. J. Direct synthesis of hydrogen peroxide from H₂ and O₂ using TiO₂-supported Au–Pd catalysts. *J. Catal.* **2005**, *236*, 69.

(57) Cattaneo, S.; Freakley, S. J.; Morgan, D. J.; Sankar, M.; Dimitratos, N.; Hutchings, G. J. Cinnamaldehyde hydrogenation using Au–Pd catalysts prepared by sol immobilisation. *Catal. Sci. Technol.* **2018**, *8*, 1677–1685.

(58) Crombie, C. M.; Lewis, R. J.; Kovačič, D.; Morgan, D. J.; Davies, T. E.; Edwards, J. K.; Skjøth-Rasmussen, M. S.; Hutchings, G. J. The Influence of Reaction Conditions on the Oxidation of Cyclohexane via the In-Situ Production of H₂O₂. *Catal. Lett.* **2021**, *151*, 164–171.

(59) Edwards, J. K.; Carley, A. F.; Herzing, A. A.; Kiely, C. J.; Hutchings, G. J. Direct synthesis of hydrogen peroxide from H₂ and O₂ using supported Au–Pd catalysts. *Faraday Discuss.* **2008**, *138*, 225.

(60) Cesana, A.; Mantegazza, M. A.; Pastori, M. A study of the organic by-products in the cyclohexanone ammoximation. *J. Mol. Catal. A: Chem.* **1997**, *117*, 367–373.

(61) Li, L.; Chen, M.; Jiang, F.-C. Design, synthesis, and evaluation of 2-piperidone derivatives for the inhibition of β -amyloid aggregation and inflammation mediated neurotoxicity. *Bioorg. Med. Chem.* **2016**, *24*, 1853–1865.

(62) Eickelberg, W.; Hoelderich, W. F. Beckmann-rearrangement of cyclododecanone oxime to ω -laurolactam in the gas phase. *J. Catal.* **2009**, *263*, 42–55.

(63) Wu, P.; Komatsu, T.; Yashima, T. Ammoximation of Ketones over Titanium Mordenite. *J. Catal.* **1997**, *168*, 400–411.